

Pyrolysis investigation of food wastes by TG-MS-DSC technique

Allouch Malika¹ · Noudem Jacques² · El Fallah Jaafar³ · Boukhlifi Fatima⁴ · Alami Mohammed¹

Received: 21 April 2015 / Revised: 7 June 2015 / Accepted: 15 June 2015 / Published online: 27 June 2015
© Springer-Verlag Berlin Heidelberg 2015

Abstract The slow pyrolysis characteristics of four food wastes, namely acorn cups (AC), acorn pericarp (AP), almond shells (AS), and nut shells (NS) were investigated by thermogravimetric (TG) analysis coupled with mass spectrometry (MS) and differential scanning calorimetry (DSC). Thermal degradation of these samples was divided into three stages corresponding to the removal of water, the devolatilization, and the formation of char; the differences in the thermal behavior of the samples are due to the differences in composition. The kinetic parameters of the process were calculated using the method of Coats-Redfern and by applying diffusion and chemical reaction kinetic models. The thermodynamic parameters were calculated for the formation of the active complex of the reagent. The main gaseous products formed during the pyrolysis were CO, CO₂, H₂O, CH₄, and C₂H₄. The comparison of the pyrolysis characteristics shows that AS was more reactive and that AC require less energy to be converted. The current investigation suggested that within the

realm of existing biomass conversion technologies, AC, AS, NS, and AP can be used as feedstock for energy recovery.

Keywords Biomass · Food waste · Energy valuation · Pyrolysis

1 Introduction

The control of energy consumption is one of the major challenges of our century in the context of sustainable development. The economic growth and the growth of the population will be translated inevitably by an increase energy needs accompanied with intensive use. With regard to the predictable depletion of the fossil resources and the environmental problems engendered by their consumption, the appeal to alternative sources of energy is inescapable to continue to satisfy the world's energy needs while protecting the environment.

Morocco, like all the countries in the world, needs to identify and to exploit all its available resources in the context of national sustainable development. Significant reserves of renewable energy forms are not yet used in this country. Among these reserves we find the biomass with its various types, biomass is in abundance and stands as the third energy resource after oil and coal [1] and due to their high reactivity and volatility, it can be easily processed to produce fuels and value-added chemicals [2]. It is a term for all organic material that stems from plants including algae, trees, and crops that are susceptible to be converted into energy [3]. Biomass is composed of three major components: cellulose, hemicelluloses, and lignin. These components usually exist in biomass in the range of 32–45 %, 19–25 %, and 14–26 % (by weight), respectively [4]. Although biomass can be converted to energy and clean fuels via thermochemical and biochemical process, the energetic valorization of biomass has received

Highlights New feedstock for alternate energy generation
Kinetic and thermodynamic parameters of pyrolysis of biomass samples
Heat requirements of biomass pyrolysis
Evolved gases during pyrolysis

✉ Allouch Malika
allouchmalika@gmail.com

¹ Laboratoire des Sciences et Métiers de l'Ingénieur, ENSAM, Moulay Ismail University, Majane 2, B.P :15290 Meknès, Morocco

² LUSAC EA-4253, Caen University, Rue Louis Aragon, BP 78, 50130 Cherbourg-Octeville, France

³ Laboratoire Catalyse and Spectrochimie, Caen University, 6, Boulevard du Maréchal Juin, 14050 Caen Cedex, France

⁴ Equip Materials and Applied Catalysis, Faculty of Science, Moulay Ismail University, Marjane 2, B.P 15290 Meknès, Morocco

considerable attention [3, 5]. One of the most controversial points in the use of biomass as an energy source is its possible competition with human food supply. Nevertheless, there are different types of biomass that fit into this definition without compromising world food supply such as food residues. In fact, almond shells, nut shells, acorn cups, and acorn pericarp are one of the main renewable energy resources available especially in an agricultural country such as Morocco. A significant advantage is that it can be converted to liquid, solid, and gaseous fuels [6] and thus can contribute to the struggle against climate changes by replacing conventional fossil fuels [1]. The use of food residues for energy production can be also an alternative solution to the problem of waste disposal [7].

Thus, this study focuses on the energetic valuation of food residues using the process of pyrolysis. Pyrolysis conversion processes are an important technological option for biofuel production and energy recovery from biomass and wastes [8]. It involves the heating of biomass in the absence of oxygen, or in a limited oxygen supply [9], it is classified into three types, namely flash, fast, and slow depending on the temperature, heating rate, and residence time. The main pyrolysis products are char, oil, and gas; char can be used as fuel, gaseous products can be used for energy production, and bio-oil can be used as a fuel or as a source of high chemical value. Our study focuses on slow pyrolysis, which occurs at a lower temperature ($<600\text{ }^{\circ}\text{C}$) with even lower heating rate of biomass ($<50\text{ }^{\circ}\text{C min}^{-1}$). It aims at charcoal production [10]. However, the process conditions for slow pyrolysis can be altered to produce significant quantities of bio-oil and gas in addition to char. Therefore, it is essential to obtain a deep knowledge of the pyrolysis of a sample of biomass in order to develop a technically and economically feasible system for its being converted to the desired fuel (liquid, gas, and solid).

The combination of thermogravimetric analysis coupled with mass spectrometry (TGA-MS) appears to give a deeper insight of the process. Some studies concerning TGA-MS of the biomass pyrolysis have been carried out [11, 12]. One of the most advantages of TGA-MS is that it is able to afford real-time and sensitive detection of evolved gases, which is an important and often a difficult task in many thermal applications [11].

Determinations of kinetic parameters such as energy activation, pre-exponential factors, and reaction order are crucial in forecasting the thermal response of samples. Determination of energy activation helps in finding out the minimum amount of energy needed to initiate a chemical change. Pre-exponential factors and the order of reaction help in calculating reaction rate. These kinetic parameters can be used in predicting the thermal behavior of the samples, and the outcome of the findings can be taken as the basis of pyrolysis studies. The reaction heat of biomass pyrolysis is an important parameter required in the heat of the pyrolysis reactor. There has been some literature concerning the determination of the

heat demand of the pyrolysis process using differential scanning calorimetry (DSC) [13, 14].

The technology of thermogravimetric analysis (TGA) coupled with mass spectrometry (MS) and differential scanning calorimetry (DSC) is able to provide the reaction kinetics the products distribution and the heat required for the process of pyrolysis.

The main purpose of this investigation is to study the slow pyrolysis of four food residues (almond shells, acorn cups, acorn pericarp, nuts shells) using TGA coupled with MS and DSC. The objectives were (a) determination of the characteristics of the main steps of the pyrolysis of biomass samples, (b) determination of kinetic model and kinetic parameters of the pyrolysis of samples, (c) qualitative characterization of the gases produced during pyrolysis, (d) quantification of energy required for the pyrolysis, and (e) comparison of the thermal characteristics of the different samples of biomass to assess the eventual use of the different samples for energy recovery.

2 Material and methods

2.1 Sample preparation

The biomass samples used in this work are collected from different regions of Morocco: acorn pericarp (AP) and acorn cups (AC) from El-Hajeb, almond shells (AS) from Meknès, and nut shells (NS) from Marrakech (Fig. 1). The compositions of the biomass samples used are given in Table 1; we performed the constituent analysis according to the method of Shiguang [15].

Before being studied, the samples of biomass were dried in an oven for 24 h at a temperature of $105\text{ }^{\circ}\text{C}$ to decrease their moisture content and facilitate their grinding. Then, they were crushed by a mortar and ground using the Pulverisette 4 Vario-Planetary Mill to a small particle size of less than $200\text{ }\mu\text{m}$ in order to have finer and homogeneous samples. Finally, they were stored in desiccators to prevent any humidity before the thermal analyses.

2.2 TGA-MS-DSC experiment

The pyrolysis of food waste samples was carried out in a SETARAM TGA-DSC apparatus (SETSYS Evolution) coupled to a Pfeiffer Vacuum mass spectrometer (OmniStar). In the first place, the pyrolysis process of each sample was carried out using a preliminary broad scan in order to identify the most prominent ions with m/z^{-1} in the range 0–300. During the experiments, about 26 mg of sample was put in a ceramic crucible pan and heated from room temperature to $900\text{ }^{\circ}\text{C}$ at a heating rate of $20\text{ }^{\circ}\text{C min}^{-1}$ in nitrogen atmosphere. We chose this heating rate to have the conditions of the slow pyrolysis ($V < 20\text{ }^{\circ}\text{C min}^{-1}$) and a good stabilization

Fig. 1 Biomass samples: acorn pericarp (AP), acorn cups (AC), almond shells (AS), nut shells (NS)



of temperature within the sample [16]. The identified signals corresponded to the mass spectra of $m/z = 16, 18, 27, 28, 29, 32, 44, 58, 60,$ and 96 which are assigned to represent $CH_4, H_2O, C_2H_4, CO, C_2H_5^+, O_2, CO_2, C_3H_6O, C_2H_4O_2,$ and $C_5H_4O_2,$ respectively.

2.3 Kinetics of pyrolysis of food residues

The data of the curve TGA were used to determine the kinetic parameters of the thermal degradation of the four food residues. The mathematical resolution of the equation of the reaction rate is performed by the integral method of Coats and Redfern [17]. This method is widely used to study the kinetics of degradation of the solid. We have adopted eight kinetic models to study the thermal decomposition of biomass samples (Table 2). Indeed, previous studies showed that the process of degradation of the biomass is governed by transport (diffusion) phenomena and chemical reactions [18, 19].

The process of pyrolysis can be represented by the following reaction schema [20]:



Table 1 Constituent analysis of biomass samples (%)

Samples	Extractives	Hemicellulose	Lignin	Cellulose	Holocellulose
AS	7	50.22	24.18	18.6	68.82
NS	4.75	55.24	26.79	13.21	68.45
AC	5	46.55	25.81	22.64	69.19
AP	4.76	56.19	36.23	2.81	59

where B_{solide} is the initial biomass and C_{solide} and D_{gaz} represent the products obtained during the pyrolysis of biomass.

The kinetic equation (Eq. 1) can be written as follows:

$$\frac{d\alpha}{dt} = f(\alpha)K(T) \tag{1}$$

$f(\alpha)$ a function whose type depends on the reaction mechanism, $K(T)$ the rate constant, T the absolute temperature, α the conversion rate, and t the time. $K(T)$ has usually the form of the Arrhenius law:

$$K(T) = A \exp\left(\frac{-E}{RT}\right) \tag{2}$$

where A is pre-exponential factor or frequency factor, E is activation energy, and R is the universal gas constant ($8314 \text{ Jmol}^{-1} \text{ K}^{-1}$).

Under a constant heating rate $\beta,$

$$\frac{dT}{dt} = \beta \tag{3}$$

After replacement and integration of Eq. 1, we get

$$g(\alpha) = \int_0^\alpha \frac{d\alpha}{f(\alpha)} = \frac{A}{\beta} \int_{T_0}^T \exp\left(\frac{-E}{RT}\right) dT \tag{4}$$

The expression $\int_{T_0}^T \exp\left(\frac{-E}{RT}\right) dT$ has no exact analytical solution, but making some substitution variables and applying Cauchy’s rule, the expression can be solved by giving

Table 2 Algebraic expressions of functions of the most common reaction mechanisms operating in solid-state reactions

Mechanism	Symbol	$f(\alpha)$	$g(\alpha)$
Chemical reaction—first order	F_1	$1-\alpha$	$-\ln(1-\alpha)$
Chemical reaction—second order	F_2	$(1-\alpha)^2$	$(1-\alpha)^{-1}-1$
Chemical reaction—third order	F_3	$(1-\alpha)^3$	$[(1-\alpha)^{-2}-1]/2$
Diffusion—one way transport	D_1	$1/2\alpha$	α^2
Diffusion—two way transport	D_2	$[-\ln(1-\alpha)]^{-1}$	$\alpha+(1-\alpha)\ln(1-\alpha)$
Diffusion—three way transport	D_3	$(2/3)(1-\alpha)^{2/3}/1-(1-\alpha)^{1/3}$	$[1-(1-\alpha)^{1/3}]^2$
Ginstling, Brounshtein equation	D_4	$(2/3)(1-\alpha)^{1/3}/1-(1-\alpha)^{1/3}$	$1-2\alpha/3-(1-\alpha)^{2/3}$
Zhuravlev, Lesokhin, Tempelman equation	D_5	$(2/3)(1-\alpha)^{5/3}/1-(1-\alpha)^{1/3}$	$[(1-\alpha)^{-1/3}-1]^2$

$$\frac{A}{\beta} \int_{T_0}^T \exp\left(\frac{-E}{RT}\right) dT = \frac{ART^2}{\beta E} \left(1 - \frac{2RT}{E}\right) \exp\left(-\frac{E}{RT}\right) \quad (5)$$

After division by T^2 and introducing the logarithm, the equation (Eq. 3) becomes

$$\ln\left[\frac{g(\alpha)}{T^2}\right] = \ln\left[\frac{AR}{\beta E} \left(1 - \frac{2RT}{E}\right)\right] - \frac{E}{RT} \quad (6)$$

Generally, the term $\frac{2RT}{E}$ can be neglected since it is too less than unity for the thermal decomposition of lignocellulosic materials [20].

So

$$\ln\frac{g(\alpha)}{T^2} = \ln\frac{AR}{\beta E} - \frac{E}{RT} \quad (7)$$

So plotting of $\ln\frac{g(\alpha)}{T^2}$ versus $\frac{1}{T}$ gives a straight line of slope $-\frac{E}{R}$, since $\ln\frac{AR}{\beta E}$ is almost constant. The expressions of $g(\alpha)$ and $f(\alpha)$ depend on the mathematical model of each mechanism of conversion. The determination of the appropriate model for the pyrolysis of different samples is based on the linear regression analysis. The plotting of $\ln\frac{g(\alpha)}{T^2}$ versus $\frac{1}{T}$ should give a straight line with a correlation coefficient close to 1; from the slope and the ordinate at the origin of this line, we have calculated E and A . The rate of conversion α is calculated from the results of the TGA using the following formula: $\alpha = \frac{m_0 - m}{m_0 - m_f}$ where m_0 , m , and m_f are respectively the initial mass, the current mass, and the final mass.

2.4 Thermodynamic parameters of biomass pyrolysis

The thermodynamic parameters of ΔH° , ΔG° , and ΔS° were calculated at $T = T_{pic}$ (T_{pic} is the derivative TG [DTG] peak temperature), since this temperature characterized the highest rate of the process [21]. The thermodynamic parameters of the pyrolysis of almond shells, nut shells, acorn cups, and acorn pericarp are presented in Table 6. These parameters were calculated by Eqs. (8)–(10) [21] using the fundamental equation

of the theory of the active complex.

$$\Delta H^\circ = E - RT \quad (8)$$

$$\Delta G^\circ = E + RT \ln \frac{K_B \times T}{h \times A} \quad (9)$$

$$\Delta S^\circ = \frac{\Delta H^\circ - \Delta G^\circ}{T} \quad (10)$$

where ΔH° and ΔS° are respectively the change of enthalpy and of entropy for the active complex formation from the reagent, ΔG° is the Gibbs free energy, K_B is the Boltzmann constant, and h is the Planck constant.

3 Results and discussion

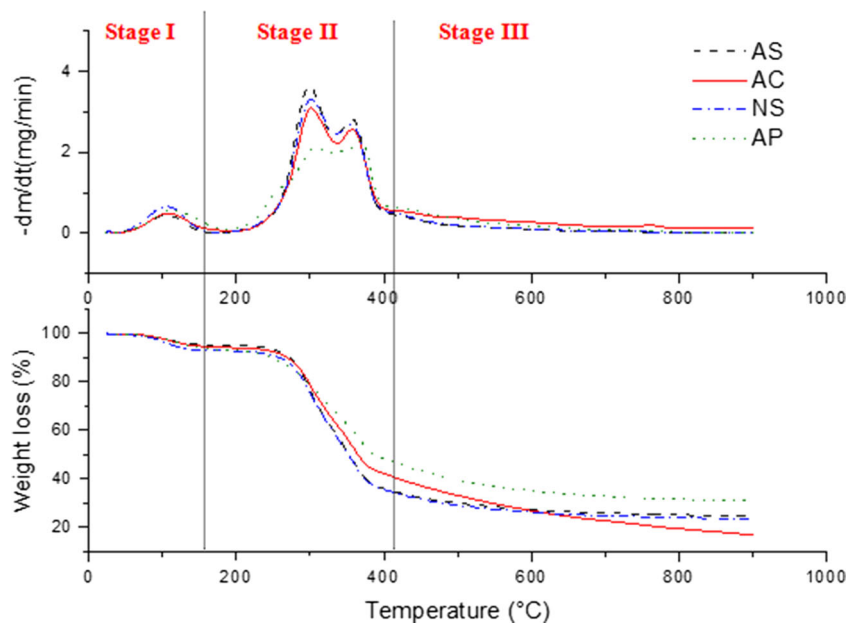
3.1 Thermogravimetric study of pyrolysis of biomass feedstocks

The purpose of the thermogravimetric analysis is to characterize the thermal behavior of the four types of waste during the pyrolysis with the aim of an energy valuation. Figure 2 shows the TGA and DTG curves of almond shells, nut shells, acorn cups, and acorn pericarp.

These curves show the typical profile of the thermal degradation of the biomass during the slow pyrolysis [22] with three stages, namely the evacuation of humidity (stage I), the devolatilization (stage II), and char formation (stage III). The main thermal characteristics derived from the curves such as the temperatures of the beginning and the end of the phenomena, the maximum weight loss, its corresponding temperatures, and the percentage of carbonaceous residue at 400 and 900 °C are summarized in the Tables 3 and 4.

We notice that the four biomass samples exhibit different behaviors during pyrolysis, in terms of mass loss, the start and the end of the reaction temperature, the degradation rate, and the temperature of maximal degradation. Since the samples were prepared in the same conditions (with the same grinding tools, the same size, the same mass, the same heating rate, and the same atmosphere), so these differences can only come

Fig. 2 TGA and DTG curves of biomass samples



from composition. In fact, the characteristics of thermal degradation of the lignocellulosic materials are strongly influenced by their chemical composition (cellulose, hemicellulose, and lignin content) [23].

The first region of mass loss is due to the removal of moisture and light volatile; this step generated a mass loss of 4.29, 5.34, 6.48, and 6.8 % respectively for AS, AC, NS, and AP samples. The highest loss for AP may be due simultaneously to its high moisture content and to its low temperature of volatile release. The devolatilization is supposed to be the step during which the pyrolysis of biomass is mainly produced; the maximum weight loss occurs during this phase. In this stage, AS, NS, and AC present the same mass loss due to their same content of holocellulose (cellulose + hemicellulose). In comparison with the biomass samples, AP presents a lower mass loss (45.28 %) due to their lower content of holocellulose (59 %). In fact, biomass is mainly composed of hemicellulose,

cellulose, and lignin; according to the study of Yang et al. [24], the mass loss of the hemicellulose, cellulose, and lignin occurs during pyrolysis in a temperature range of 220–315, 315–400, and 160–900 °C, respectively.

We notice that the devolatilization begins at temperatures of 197, 198, 193, and 178 °C for AS, AC, NS, and AP samples, respectively. These variations in the temperatures at the beginning of degradation of the biomass were related to differences in chemical and elemental composition of samples as described by some authors [25]. During this stage, two processes of decomposition corresponding to the degradation of the hemicellulose and the cellulose are observed; DTG curve shows two regions; the first exhibits peaks at temperatures of 299, 301, 301, and 308 °C for AS, AC, NS, and AP, respectively; this region may be generated by the degradation of the hemicellulose and a part of the lignin. The second region exhibits peaks at temperatures of 357, 357, 356, and 368 °C

Table 3 Main thermal characteristics of devolatilization of biomass samples

Sample	Temperature range (°C)	T_{pic}^a (°C)	V_{pic}^b (mg min ⁻¹)	% R.C ^c -400	Mass loss (%)	$R_M \cdot 10^3$ (% s ⁻¹ °C ⁻¹)
AS	197–400	299	3.65	35.72	59.08	1.3
		357	2.82			
AC	198–401	301	3.096	41.81	52.03	1.1
		357	2.56			
NS	193–409	301	3.312	35.25	57.83	1.2
		356	2.68			
AP	178–404	308	2.12	48.16	45.28	0.7
		368	2.32			

^a Temperature of maximum rate loss

^b Maximum rate loss

^c Carbonaceous residue

Table 4 Main thermal characteristics of char formation

Sample	Temperature range (°C)	V_m^a (mg min ⁻¹)	% R.C ^b -900
AS	400–900	0.11	24.79
AC	401–900	0.26	16.95
NS	409–900	0.11	23.69
AP	404–900	0.19	31.22

^a Average rate loss,

^b Carbonaceous residue

for the four samples shown before, respectively. This region may be due to the decomposition of the cellulose and a proportion of the lignin. The devolatilization almost ends at a temperature of 400 °C, acorn pericarp has the highest percentage of the carbon residue (48.16 %), and this is due to their high lignin content (36.24 %). The mass losses in the third phase are much lower than those of the second (11.28–25.09 %). These losses can result from the pyrolysis of the lignin, auto-gasification, or from secondary reactions. The highest residue is noticed at the level of the acorn pericarp (31.22 %), since hemicellulose and lignin mainly degrade giving coal, while inorganic materials catalyze its formation [26]; thus, we explain this by the fact that the acorn pericarp contains more lignin or it may also contain more mineral materials.

From the maximum loss rate and the corresponding temperature, we calculated the reactivity of samples using the method proposed by Ghetti et al. [27]:

$$R_M = \sum \frac{V_{pic}}{T_{pic}} \quad (11)$$

The parameter $10^3 R_M$ is calculated for each sample. The obtained results are reported in Table 3.

According to the value of R_M , the biomass samples are classified in the following order: AS > NS > AC > AP. The

obtained values (0.7–1.3 % s⁻¹ °C⁻¹) are superior to those obtained by Munir et al. [28] during the pyrolysis of four various food wastes and to those of El may et al. [29] during the pyrolysis of five different residues of the date palm.

3.2 Kinetic parameters

According to the results of the TGA and DTG, we noticed that the pyrolysis of our samples goes through three main stages: degradation of hemicellulose, degradation of cellulose, and formation of char. For each step, we determined the appropriate kinetic model and its parameters (Table 5).

The results of the TGA were examined using diffusion and chemical reaction mechanisms; the best correlation is obtained with the models based on the chemical reaction mechanism of the first and the second order (F_1 , F_2) and diffusion mechanism (D_3 , D_5). In the literature, these models are the most appropriate for describing the thermal degradation of lignocellulosic materials [18, 19]. The kinetic parameters characterizing the process of pyrolysis of biomass samples differ from a stage to another and from a sample to another; the devolatilization of our samples occurs at two stages; from Table 5, we notice that the diffusion model D_3 is the most suitable for AP and AC in the first step and that of the first order chemical reaction for AS and NS, and the second stage is best described by the model second order chemical reaction F_2 for the four samples. F_2 is the most appropriate model for the formation of char for AP, AS, and NS; however, the formation of char for AC is governed by D_5 . The mechanisms governing the pyrolysis of biomass differ from a sample to another; indeed, Jeguirim et al. [30] studied the pyrolysis of five types of biomass; they found that the mechanisms of the first order chemical reaction (F_1) and of diffusion (D_1 , D_2 , D_3 , D_4) describe the devolatilization while the third order chemical reaction mechanism (F_3) is more reasonable for the formation of the char. Vlaev et al. [19] found that the thermal

Table 5 The kinetic characteristics of the pyrolysis of the biomass samples

Sample	Temperature range (°C)	Frequency factor (s ⁻¹)	Activation energy (kJ mol ⁻¹)	R^2	Mechanism
AS	197–330	1.05×10^{10}	130.69	0.98	F_1
	330–400	1.46×10^{26}	333.25	0.98	F_2
	400–900	2.92×10^2	72.15	0.89	F_2
AC	198–331	1.32×10^{20}	251.84	0.98	D_3
	33–401	3.55×10^{25}	326.94	0.97	F_2
	400–900	5.35×10^2	100.53	0.91	D_5
NS	192.79–332	6.08×10^{10}	132.84	0.99	F_1
	332–409	5.74×10^{24}	309.74	0.98	F_2
	409–900	50.97×10^3	91.59	0.93	F_2
AP	178–330	5.72×10^{13}	180.93	0.98	D_3
	330–404	3.84×10^{23}	304.73	0.97	F_2
	404–900	1.43×10^3	82.64	0.91	F_2

Table 6 Thermodynamic parameters of biomass samples at the maximum differential mass conversion

Sample	E (kJ mol ⁻¹)	A (s ⁻¹)	ΔH (kJ mol ⁻¹)	ΔG (kJ mol ⁻¹)	ΔS (J mol ⁻¹)
AS ^a	130.69	1.05×10^{10}	126	164	-66
AS ^b	333.25	1.46×10^{26}	328	176	241
AC ^a	251.84	1.32×10^{20}	247	174	127
AC ^b	326.94	3.55×10^{25}	322	177	30
NS ^a	132.84	6.08×10^{10}	128	158	-52
NS ^b	309.74	5.74×10^{24}	305	170	215
AP ^a	180.93	5.72×10^{13}	176	188	-20.65
AP ^b	304.73	3.84×10^{23}	299	176	192

^a and ^b are respectively the first and the second peak in DTG curve

degradation of the rice husk under an inert atmosphere is described by the diffusion mechanism D₄.

By comparing the kinetic parameters calculated using the models that have given the best correlation, we found that the activation energy of the pyrolysis steps of the four samples is classified as follows: $E_{V2} > E_{V1} > E_{ch}$; E_{V1} and E_{V2} are respectively the activation energies of the first and second devolatilization stage; E_{ch} is the activation energy associated to the formation of char. The same classification is obtained for the pre-exponential factors. The resulting classification is logical since it is well known that cellulose has the highest activation energy during the thermal degradation in comparison with the hemicelluloses and lignin [30]. Consequently, samples having high contents of cellulose have higher activation energy values. The activation energies of the three main stages of pyrolysis are respectively (180.93 kJ mol⁻¹; 304.73 kJ mol⁻¹; 82.64 kJ mol⁻¹), (130.69 kJ mol⁻¹; 333.25 kJ mol⁻¹; 72.15 kJ mol⁻¹), (251.84 kJ mol⁻¹; 326.94 kJ mol⁻¹; 100.53 kJ mol⁻¹) et (132.84 kJ mol⁻¹, 309.74 kJ mol⁻¹; 91.59 kJ mol⁻¹) for AP, AS, AC, and NS. The obtained values are higher than those found by Jeguirim et al. [30] and close to those found by Vlaev et al. [19]. The development of economically and technically feasible systems for thermochemical conversion of food waste into energy requires a fundamental understanding of their thermal properties and kinetics degradation.

3.3 Thermodynamic parameters of biomass pyrolysis

The change of Gibbs free energy ΔG° reflects the total energy increase of the system at the approach of the reagents and the formation of the activated complex. This energy is influenced by two thermodynamic properties, the changes of enthalpy ΔH° and entropy ΔS° of activated complex formation. The change of activation enthalpy shows the energy differences between the activated complex and the reagents. If this difference is small, the formation of activated complex is favored, because the potential energy barrier is low.

The change in entropy reaction reflects how near the system is to its own thermodynamic equilibrium. Low activation

entropy means that the material has just gone through some kind of physical or chemical aging process, bringing it to a state near its own thermodynamic equilibrium. In this situation, the material showed poor reactivity, increasing the time necessary to form the activated complex. On the other hand, when high activation entropy values are observed, the material is far from its own thermodynamic equilibrium. Thus, the reactivity is high and the system can react faster to produce the activated complex, and consequently, short reaction times are observed [31]. The entropy measures the disorder in a system. The negative values of entropies of the formation of the activated complex mean that the activated complex can be characterized by a much higher degree of arrangement, in the first stage of devolatilization, except that the decomposition of acorn cups all values of ΔS° were negative, which illustrated that the activated complex had more organized structure compared to the initial substance. Contrariwise, the values of the ΔS° of the second stage of devolatilization were positive for all samples which illustrated that the activated complex of this stage was more disordered. We also notice the increase of the entropy at the second stage, which indicated the increase of the reactivity of the samples at this stage and of the rate of decomposition to produce the activated complex. So, the samples were less reactive in the first zone than the second. The changes of entropies agreed with the frequency factors.

Based on Table 6, the activation energies and the enthalpies of the second stage of devolatilization were greater than those of the first stage, so more heat energy was required for the second stage than the first in order to dissociate the bonds of reagents.

3.4 Analysis of the gases produced during pyrolysis

The most attractive advantage of the TGA-MS is that it allows to follow in parallel the evolutions of the mass according to the temperature and the chemical composition of the emitted vapors [32].

The identification of fragments is based on literature data and on the chemical structure of biomass. The ion current signal is generated when there is a compound or an atom that

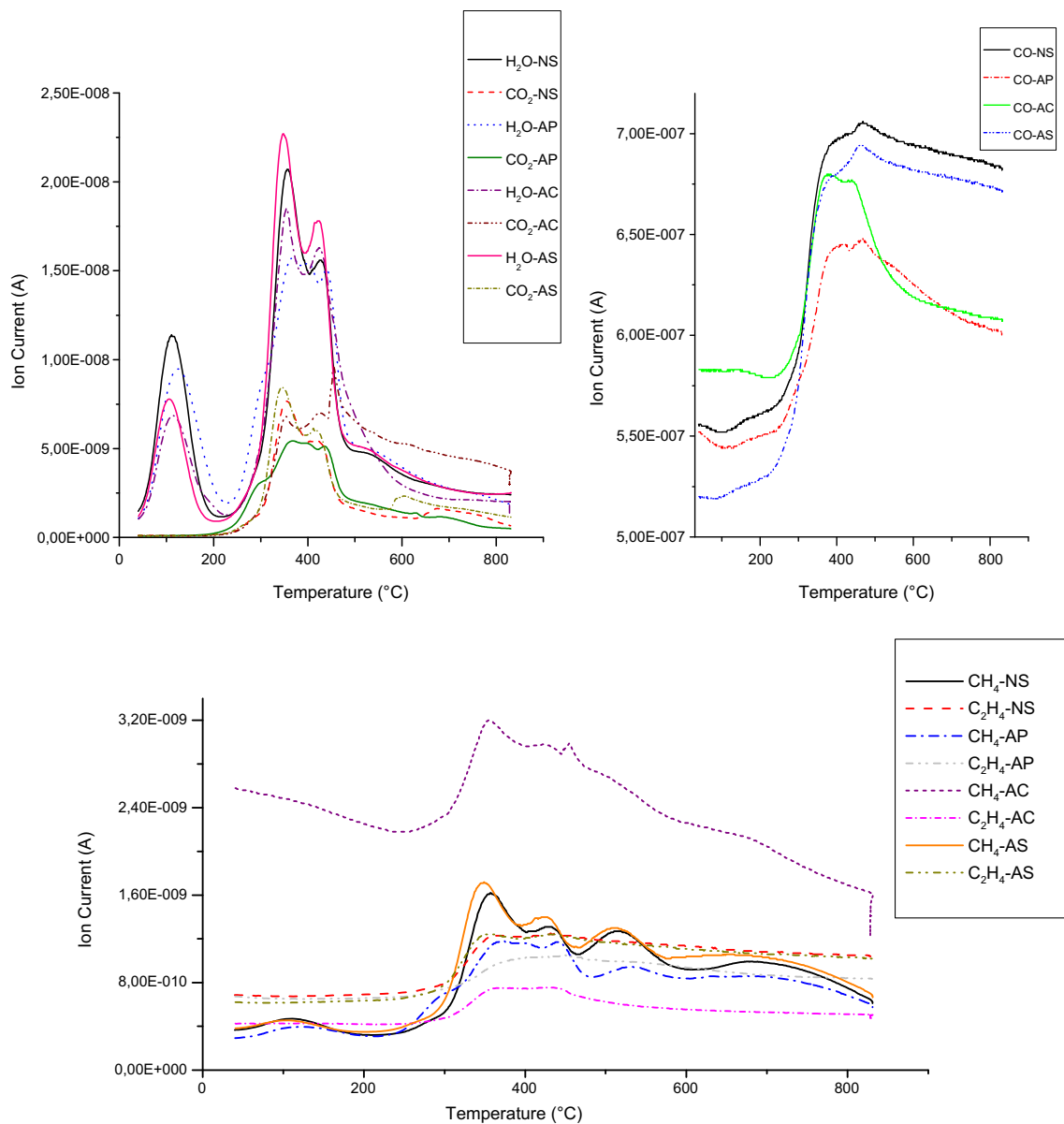


Fig. 3 a, b, c Evolution of CO, H₂O, CO₂, CH₄, and C₂H₄ during the pyrolysis of biomass samples

has been created by the ionization of molecules in the gas phase; consequently, the study of the evolution of gases emitted during the pyrolysis versus temperature of the various types of waste is realized by analyzing the changes of the ionic current obtained by mass spectrometry.

The profiles of the changes in ion current as a function of the temperature of the four samples of biomass are shown in Figs. 3 and 4.

The main products detected during pyrolysis are CO, CO₂, H₂O, O₂, and some light hydrocarbons (CH₄, C₂H₄, C₂H₅⁺). A relatively significant amount of CO and H₂O are detected because of the large number of hydroxyl groups and oxygen atoms present in the biomass samples (cellulose, hemicellulose, and lignin). We note that the majority of gases generated in the temperature range of 250–500 °C and that all samples

have the same gas evolution profile with differences just at the peak intensity.

Almond shells and nut shells present the same profile with almost the same peaks intensities. At temperatures below 200 °C, there is just the production of H₂O; its peaks coincide with those of the DTG curve during sample drying step. The release of H₂O and CO₂ takes place between 250 and 500 °C; these two gases have two peaks in this range around 340 and 405 °C. H₂O was produced on all the interval of decomposition of the biomass, what indicates its provenance from different origins; the peak obtained at approximately 105 °C is due to the liberation of absorbed water, while the peaks beyond 200 °C correspond to the water formed during the decomposition of hemicellulose, cellulose, and lignin [12]. CO is produced between 300 and 600 °C; CO and CO₂ are also

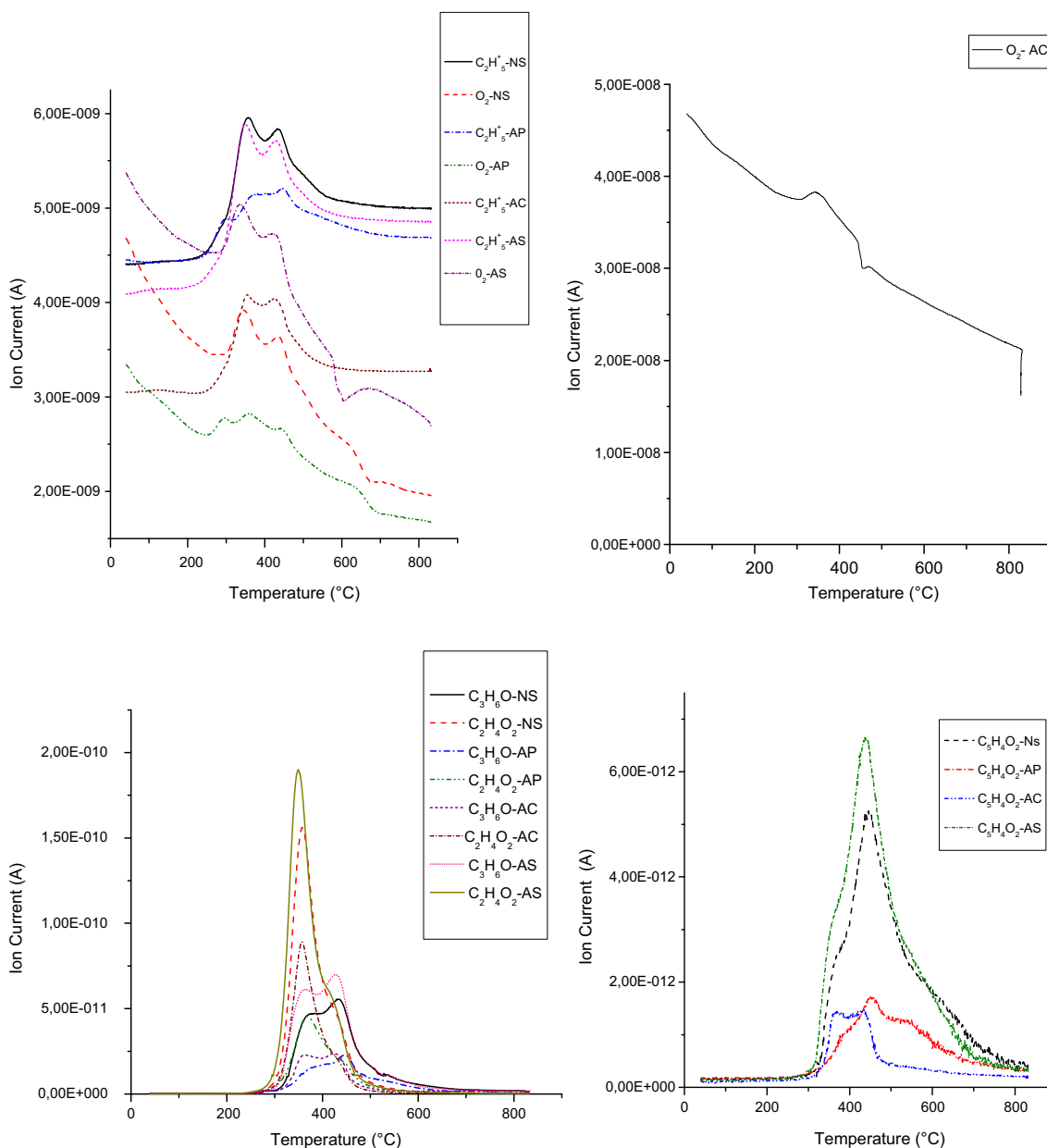


Fig. 4 a, b, c, d Evolution of C₅H₄O₂, C₃H₆O, C₂H₄O₂, C₂H + 5, and O₂ during the pyrolysis of biomass samples

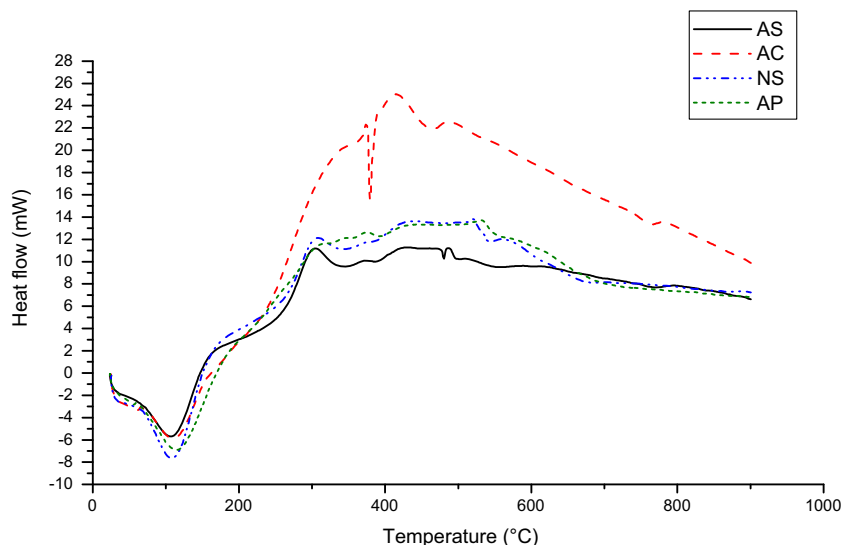
formed from the degradation of cellulose, hemicellulose, and lignin. The evolution of C₂H₅⁺ and O₂ occurs between 300 and 500 °C and that of C₃H₆O and C₂H₄O₂ between 300 and 500 °C; C₃H₆O is mainly due to the degradation of cellulose [12]. C₅H₄O₂ was detected between 300 and 700 °C for NS and AS, between 300 and 500 °C for AC, and between 300 and 680 °C for AP. This shows that C₅H₄O₂ is derived from the degradation of lignin. The production of C₂H₄ occurs between 300 and 480 °C, so it results from the degradation of the cellulose. The release of CH₄ happens between 200 and 600 °C; at low temperatures, CH₄ comes from the degradation of the cellulose and hemicelluloses [33]. At high temperatures, CH₄ is mainly produced by the cracking of the methoxyl

groups [34]. The gases detected during the pyrolysis of the four wastes can be used to warm the reactor of pyrolysis or to produce the heat and the electricity for other processes.

3.5 The energy required for the pyrolysis biomass feedstocks

Differential scanning calorimetry is used to quantify the amount of energy required for the pyrolysis of the four types of wastes; the heat required for the pyrolysis reactions is an essential parameter in the design of a pyrolysis reactor, the specification of operating parameters, the study of the energy balance, and the potential of the energy valuation of waste in

Fig. 5 DSC curves of biomass samples



fuel by pyrolysis process. The pyrolysis is an endothermic reaction; the heat of reaction must be supplied by an external source. According to the TG-MS analysis, the combustion of gases stemming from this degradation (CH₄, C₂H₄, CO, CO₂) can supply the energy needed.

The heat required to pyrolyze the biomass contains two-component equation (Eq. 12), the heat required for heating the biomass at the temperature at which pyrolysis occurs and the heat required for the pyrolysis itself.

$$Q = m_b C_{p,b}(T_r - T_i) + m_b \Delta H_r \tag{12}$$

where Q is the heat requirement of biomass pyrolysis, m_b is the mass of biomass, $c_{p,b}$ is the specific heat capacity of biomass, T_r is the temperature at which pyrolysis occurs, T_i is the initial temperature, and ΔH_r is the reaction heat of pyrolysis.

The DSC curves of the four samples (Fig. 5) exhibit the variation of heat flow (mW) as a function of the temperature during the thermal decomposition of samples within the temperature range of 40 to 900 °C. The endothermic peaks obtained around 105 °C are due to the evaporation of the moisture contained in the samples [35].

For the DSC curve in Fig. 5, the data on Y coordinate is

$$\frac{dQ}{dT} = m_s C_{p,s} \frac{dT}{dt} + m_s \Delta H_r \tag{13}$$

The integration of this curve equation (Eq. 14) provides the heat required for pyrolysis

$$\frac{Q}{m_{s,0}} = \int_0^t \frac{m_s C_{p,s} \frac{dT}{dt} + m_s \Delta H_r}{m_{s,0}} dt \tag{14}$$

where $m_{s,0}$ is the initial mass of sample, and $c_{p,s}$ and m_s are respectively the specific heat capacity and the mass of sample during TGA-DSC-MS experiment.

The analysis of the heat flow information was performed by dividing the data into two zones. The first zone represents the energy of the evacuation of humidity and of the heating of samples to the temperature at which the pyrolysis occurs; the second zone represents the energy of thermal decomposition of the samples. The TGA study showed that the thermal degradation begins at temperatures of 197, 19, 193, and 178 °C respectively for AS, AC, NS, and AP and ends at about 400 °C.

Table 7 The energy required for the pyrolysis of the four biomass samples

Sample	Temperature (°C)	Energy required (kJ kg ⁻¹)	Total energy required (kJ kg ⁻¹)
AS	40–197	30	54.30
	197–400	24.30	
AC	40–198	30.23	43.23
	198–400	13	
NS	40–192.79	39.18	58.04
	192.79–400	18.86	
AP	40–178	41	81
	178–400	40	

The energy required for each zone is obtained by integrating the heat flow curve using software supplied by the manufacturer of the DSC. Table 7 shows the found results.

From these results, we find that the energy required for the pyrolysis varies from one sample to another; acorn pericarp requires more energy (81 kJ kg^{-1}) in comparison with other samples. The heat required to remove moisture from the samples is significantly higher than that required for the thermal decomposition; similar results were reported by Fasina and Littlefield [13] for the shells of pecans [36] and Park et al. for wood cellulose fibers. Based on the values of the energy required for the removal of moisture, samples can be classified as follows: $AP > NS > AC > AS$; the same sequencing is obtained based on mass loss values in this region; this shows that the sample having the high moisture content requires more energy. So moisture content is an important criterion to be considered for the valuation of biomass by pyrolysis.

4 Conclusion

Food residues namely acorn cups (AC), acorn pericarp (AP), almond shells (AS), and nut shells (NS) were evaluated as a potential feedstock for slow pyrolysis process for energy recovery using TGA-DSC-MS. The following conclusions can be drawn from this study:

- TG and DTG results showed that the pyrolysis of the samples was represented by three successive steps: The first step corresponded to the evaporation of moisture, the second step to the devolatilization. It occurs at two stages: the first stage corresponds to degradation of hemicellulose, it is well described by diffusion model D_3 for AP and AC and by chemical reaction model F_1 for AS and NS; the second stage by the chemical reaction model F_2 for the four sample; and the third step corresponded to char formation characterized by low weight loss rate. It is well described by chemical reaction model F_2 for AP, AS, and NS and by diffusion model D_5 for AC.
- The MS results showed that CO , CO_2 , H_2O , CH_4 , and C_2H_4 were the main gaseous products released during the pyrolysis of the samples; such gases could be used to warm the reactor of pyrolysis or to produce the heat and the electricity for other processes.
- The DSC results showed that the moisture content is an important criterion to be considered for the valuation of the biomass by pyrolysis.
- Comparing the pyrolysis behavior of the sample, we found that AS was the most reactive one and that AC need more energy during pyrolysis.
- The kinetic parameters of the main steps of pyrolysis and the thermodynamic parameters for the formation of the active complex of the reagent during pyrolysis were

calculated. The obtained values are useful for the configuration and the designing of the suitable pyrolysis reactor.

Acknowledgments The authors are very thankful to the laboratory LUSAC, Caen University, for providing the facilities and for its constant encouragement. The authors are also grateful to Mr. Gualous Hamid for his precious help.

References

1. Radmanesh R, Courbariaux Y, Chaouki J, Guy C (2006) A unified lumped approach in kinetic modelling of biomass pyrolysis. *Fuel* 85:1211–1220
2. Phukan MM, Chutia RS, Konwar BK, Kataki R (2011) Microalgae chlorella as a potential bio-energy feedstock. *Appl Energy* 88: 3307–3312
3. McKendry P (2002) Energy production from biomass (part 1): overview of biomass. *Bioresour Technol* 83:37–46
4. Brown R (2009) Biochar production technology. In: Lehmann J, Joseph S (Eds.) *Biochar for environmental management*, Sterling, Virginia, USA, pp 227–144
5. Chen Q, Yang R, Zhao B, Li Y, Wang S, Wu H, Zhuo Y, Chen C (2014) Investigation of heat of biomass pyrolysis and secondary reactions by simultaneous thermogravimetry and differential scanning calorimetry. *Fuel* 134:467–476
6. Yaman S (2004) Pyrolysis of biomass to produce fuels and chemical feedstocks. *Energy Convers Manag* 45:651–671
7. Zabaniotou AA, Kalogiannis G, Kappas E, Karabelas AJ (2000) Olive residues (cuttings and kernels) rapid pyrolysis product yields and kinetics. *Biomass Bioenergy* 18:411–420
8. Haydary J, Jelemensky L, Gasparovic L, Markos J (2012) Influence of particle size and kinetic parameters on tire pyrolysis. *Anal Appl Pyrolysis* 97:73–79
9. Antonakou E, Lappas A, Nilsen MH, Bouzga A, Stöcker M (2006) Evaluation of various types of Al-MCM-41 materials as catalysts in biomass pyrolysis for the production of bio-fuels and chemicals. *Fuel* 85:2202–2212
10. Ballerini D (2006) *Les biocarburants, état des lieux, perspectives et enjeux du développement*. Technip, Paris
11. Huang YF, Kuan WH, Chiueh PT, Lo SL (2011) Pyrolysis of biomass by thermal analysis–mass spectrometry (TA–MS). *Bioresour Technol* 101:1968–1973
12. Gómez CJ, Mészáros E, Jakab E, Velo E, Puigjaner L (2007) Thermogravimetry/mass spectrometry study of woody residues and an herbaceous biomass crop using PCA techniques. *Anal Appl Pyrolysis* 80:416–426
13. Fasina O, Littlefield B (2012) TG-FTIR analysis of pecan shells thermal decomposition. *Fuel Process Technol* 102:61–66
14. He F, Yi W, Bai X (2006) Investigation on caloric requirement of biomass pyrolysis using TG–DSC analyzer. *Energy Convers Manag* 47:2461–2469
15. Shiguang L, Shaoping X, Shuqin L, Yang C, Qinghua L (2004) Fast pyrolysis of biomass in free-fall reactor for hydrogen-rich gas. *Fuel Process Technol* 85:1201–1211
16. Chouchene A (2010) *Etude expérimentale et théorique de procédés de valorisation de sous produits oléicoles par voies thermique et physico-chimique*. Doctoral thesis of the university of High Alsace, pp 23
17. Coats AW, Redfern JP (1964) Kinetic parameters from thermogravimetric data. *Nature* 201:68–69
18. Gil MV, Casal D, Pevida C, Pis JJ, Rubiera F (2010) Thermal behaviour and kinetics of coal/biomass blends during co-combustion. *Bioresour Technol* 101:5601–5608

19. Vlaev L, Markovska I, Lyubchev L (2003) Non-isothermal kinetics of pyrolysis of rice husk. *Thermochim Acta* 406:1–7
20. Brown M E (2001) Introduction to thermal analysis: techniques and applications. 2nd ed. Springer
21. Kim YS, Kim SH (2010) Investigation of thermodynamic parameters in the thermal decomposition of plastic waste–waste lube oil compounds. *Environ Sci Technol* 44:5313–5317
22. Órfão JJM, Antunes FJA, Figueiredo JL (1999) Pyrolysis kinetics of lignocellulosic materials—three independent reactions model. *Fuel* 78:349–358
23. Shafizadeh F, Bradbury AGW (1979) Thermal degradation of cellulose in air and nitrogen at low temperatures. *Appl Polym Sci* 23:1431–1442
24. Yang HP, Yan R, Chen HP, Lee DH, Zheng CG (2007) Characteristics of hemicelluloses, cellulose and lignin pyrolysis. *Fuel* 86:1781–1788
25. Mansaray KG, Ghaly AE (1998) Thermal degradation of rice husks in nitrogen. *Bioresour Technol* 65:13–20
26. Philpot CW (1970) Influence of mineral content on the pyrolysis of plant materials. *For Sci* 16:4761–4771
27. Ghetti P, Ricca L, Angelini L (1996) Thermal analysis of biomass and corresponding pyrolysis products. *Fuel* 75:565–573
28. Munir S, Daood SS, Nimmo W, Cunliffe AM, Gibbs BM (2009) Thermal analysis and devolatilization kinetics of cotton stalk, sugar cane bagasse and shea meal under nitrogen and air atmospheres. *Bioresour Technol* 100:1413–1418
29. El may Y, Jeguirim M, Dorge S, Trouvé G, Said R (2012) Study on the thermal behavior of different date palm residues: characterization and devolatilization kinetics under inert and oxidative atmospheres. *Energy* 44:702–709
30. Jeguirim M, Bikai J, Elmay Y, Limousy L, Njeugna E (2014) Thermal characterization and pyrolysis kinetics of tropical biomass feedstocks for energy recovery. *Energy Sustain Dev* 23:188–193
31. Ruvolo-Filho A, Curti PS (2006) Chemical kinetic model and thermodynamic compensation effect of alkaline hydrolysis of waste poly (ethyleneterephthalate) in nonaqueous ethylene glycol solution. *Ind Eng Chem Res* 45:7985–7996
32. Ateş F, Pütün AE, Pütün E (2006) Pyrolysis of two different biomass samples in a fixed-bed reactor combined with two different catalysts. *Fuel* 85:1851–1859
33. zveren U, zdoğan ZS (2013) Investigation of the slow pyrolysis kinetics of olive oil pomace using thermo-gravimetric analysis coupled with mass spectrometry. *Biomass Bioenergy* 58:168–179
34. Jakab E, Fdix O, Tiii F (1997) Thermal decomposition of milled WOCA lignins studied by thermogravimetry/mass spectrometry. *Anal Appl Pyrolysis* 40–41:171–186
35. Fang H, Weiming Y, Xueyuan B (2006) Investigation on calorific requirement of biomass pyrolysis using TG-DSC analyzer. *Energy Convers Manage* 47:2461–2469
36. Park S, Venditti R, Jameel H, Pawlak J (2007) Studies of the heat of vaporization of water associated with cellulose fibers characterized by thermal analysis. *Cellulose* 14:195–204